Journal of Organometallic Chemistry 693 (2008) 2052–2060

Contents lists available at ScienceDirect

Journal of Organometallic Chemistry

journal homepage: www.elsevier.com/locate/jorganchem

Detailed mechanisms on insertion of *cis*-2-butene into the Zr–H bond of Cp_2ZrH_2: A DFT study

Siwei Bi [a,b,*], Xiaojian Kong [a], Yanyun Zhao [a], Xiaoran Zhao [a], Qingming Xie [a]

[a] College of Chemistry Science, Qufu Normal University, Qufu, Shandong 273165, PR China
[b] State Key Laboratory of Physical Chemistry of Solid Surfaces, Xiamen University, PR China

ARTICLE INFO

Article history:
Received 13 November 2007
Received in revised form 28 February 2008
Accepted 6 March 2008
Available online 18 March 2008

Keywords:
Cp_2ZrH_2
cis-2-Butene
Olefin insertion
β-Hydrogen elimination
Agostic interaction

ABSTRACT

The detailed mechanisms for reaction of Cp_2ZrH_2 with *cis*-2-butene were explored with the aid of density functional theory calculations. Two possible pathways for olefin insertion into the Zr–H of Cp_2ZrH_2 were proposed. One is the side-insertion and the other is the central-insertion. The central-insertion is theoretically predicted to be more favorable kinetically than the side-insertion. It is revealed that formation and cleavage of Zr···H–C agostic interaction and β-hydrogen elimination are requisite steps in addition to the olefin insertions. The side-agostic and the central-agostic interactions are found to be involved in some intermediates. The former agostic is less stable than the latter, which plays a role in describing which path is preferred.

© 2008 Elsevier B.V. All rights reserved.

1. Introduction

Bent metallocene catalysts for polymerization of ethylene, propene, butene and other olefins are a topic of intense current interest and hold much attention of many people. For olefin polymerization, olefin insertion into a metal–carbon bond plays an important role in chain propagation while β-hydrogen elimination serves as a chain-termination step. Electrophilic d^0 group 4 bent metallocenes, such as $Cp_2Zr(CH_3)_2$ (Cp = η^5-cyclopentadienyl), are precursors for alkene polymerization catalysts [1,2] and now enter commercial application [3]. Olefin insertion into a metal–hydride bond and the related β-hydrogen elimination from a metal alkyl are also fundamental transformations in organometallic chemistry [4–7]. Furthermore, both olefin insertion and β-hydrogen elimination are requisite steps in a variety of important catalytic reaction [8]. Thus, a detailed understanding of the mechanisms on olefin insertion and β-hydrogen elimination processes is of importance in organometallic chemistry and catalysis.

Chirik and Bercaw confirmed that addition of *cis*-2-butene to a toluene-d_8 solution of $Cp^*_2ZrH_2$ afforded a zirconocene *n*-butyl hydride complex $Cp^*_2ZrH(CH_2CH_2CH_2CH_3)$ (Eq. (1)) [9]. The zirconocene *sec*-butyl hydride intermediate afforded by direct insertion of *cis*-2-butene was not been detected, even when the reaction was monitored at −90 °C. That means this reaction experiences isomerization from zirconocene *sec*-butyl hydride intermediate to zirconocene *n*-butyl hydride product. Many theoretical mechanistic studies on olefin insertion into the metal–hydrogen bond have been reported [10,11]. However, to our knowledge, the detailed theoretical mechanistic exploration on *cis*-2-butene insertion into the Zr–H bond of $Cp^*_2ZrH_2$, accompanied by isomerization of the zirconocene *sec*-butyl hydride intermediate to give its *n*-butyl isomer, has not been undertaken

(1)

In the coordinatively unsaturated 16-electron Cp_2ZrH_2 complexes, eight out of the available nine metal valence orbitals are used for making metal-to-ligand bonds. The remaining ninth empty orbital in principle could either occupy a central position between the two Zr–H bonds or be aligned laterally. Accordingly, two possible olefin insertion modes can be suggested. One insertion, defined here as "central-insertion", is from the central position of the two Zr–H bonds. The other, defined here as "side-insertion", is from the outside of either Zr–H (Scheme 1). Two types of agostics are involved in the process, defined here as "central-agostic" and "side-agostic", respectively, as shown in Scheme 2. The Zr···H–C moiety lies in between the Zr–H and Zr–C bonds in

* Corresponding author. Address: College of Chemistry Science, Qufu Normal University, Qufu, Shandong 273165, PR China. Fax: +86 537 4456305.
E-mail address: siweibi@126.com (S. Bi).

0022-328X/$ - see front matter © 2008 Elsevier B.V. All rights reserved.
doi:10.1016/j.jorganchem.2008.03.004

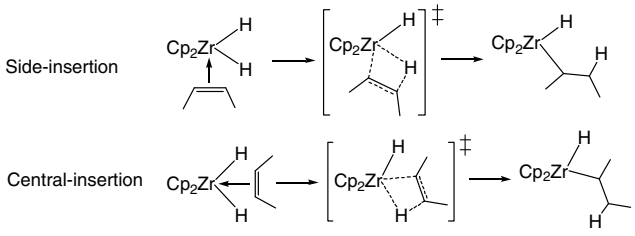

Scheme 1.

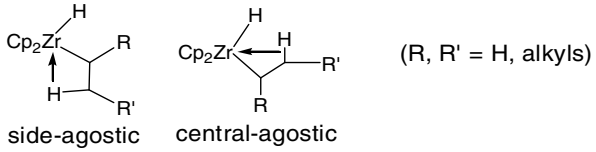

Scheme 2.

the first type and the Zr···H–C lies on the outside of the Zr–C bond in the second type. For a 16-electron dimethylzirconocene, Cp_2ZrMe_2, some early discussion confirmed clearly that its LUMO is laterally extending in the major σ-ligand plane [10–12]. As a result, a donor ligand is expected to enter the molecule from the side rather than the central position between the σ-ligands under kinetic control. This was demonstrated experimentally for a number of cases [13–20]. The insertion of olefin into the Zr–H bond of Cp_2ZrHCl was theoretically investigated and the 'central-insertion" was confirmed to be favored kinetically [21,22]. In this work, our goal is to theoretically investigate how *cis*-2-butene inserts into the Zr–H of Cp_2ZrH_2 (side-insertion or central-insertion?) and how the subsequent isomerization occurs with the aid of density functional theory calculations.

2. Computational details

Full molecular geometry optimizations have been carried out at the Becke3LYP (B3LYP) level of density functional theory (DFT) [23–25]. Frequency calculations at the same level of theory have also been performed to identify all stationary points as minima (zero imaginary frequencies) or transition states (only one imaginary frequency). The effective core potentials (ECPs) of Hay and Wadt with double-ζ valence basis sets (LanL2DZ) [26] were used to describe Zr. Polarization functions were added for C (ζ(d) = 0.8), H (ζ(d) = 0.11) [27]. The 6-31G basis set was used for all the atoms except Zr [28,29]. The transition states involved were

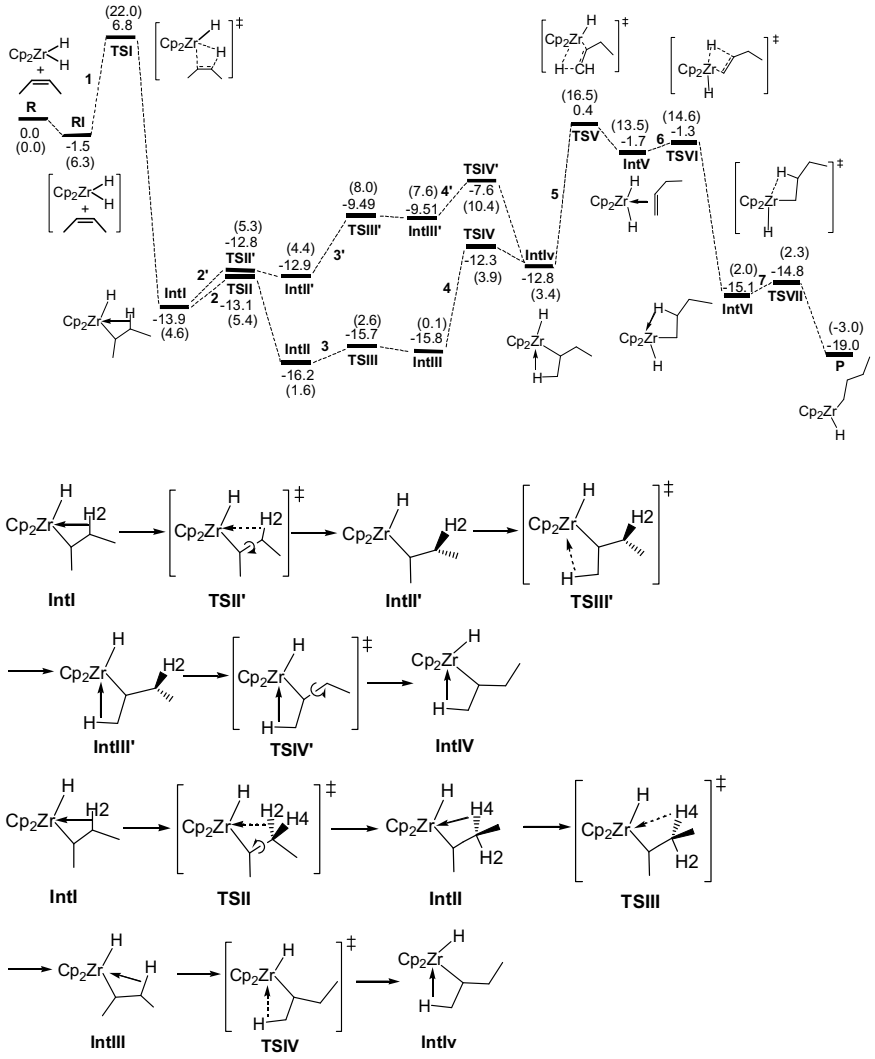

Fig. 1. Potential energy profile for the side-insertion of *cis*-2-butene into the Zr–H of Cp_2ZrH_2. The free energies are given in bracket. The energies are given in kcal/mol.

checked by intrinsic reaction coordinate (IRC) analysis [30,31]. All the calculations were performed with the GAUSSIAN 98 software package [32]. In all the energy profiles, the calculated electronic energies were used to describe the energetic aspects. To simplify calculations, we substitute Cp for Cp^*. In this model, the influence of the methyl groups of Cp^* on the detailed mechanism is not considered. Our goal is not to determine the accurate energy values but to explore the reaction paths. The computational method and

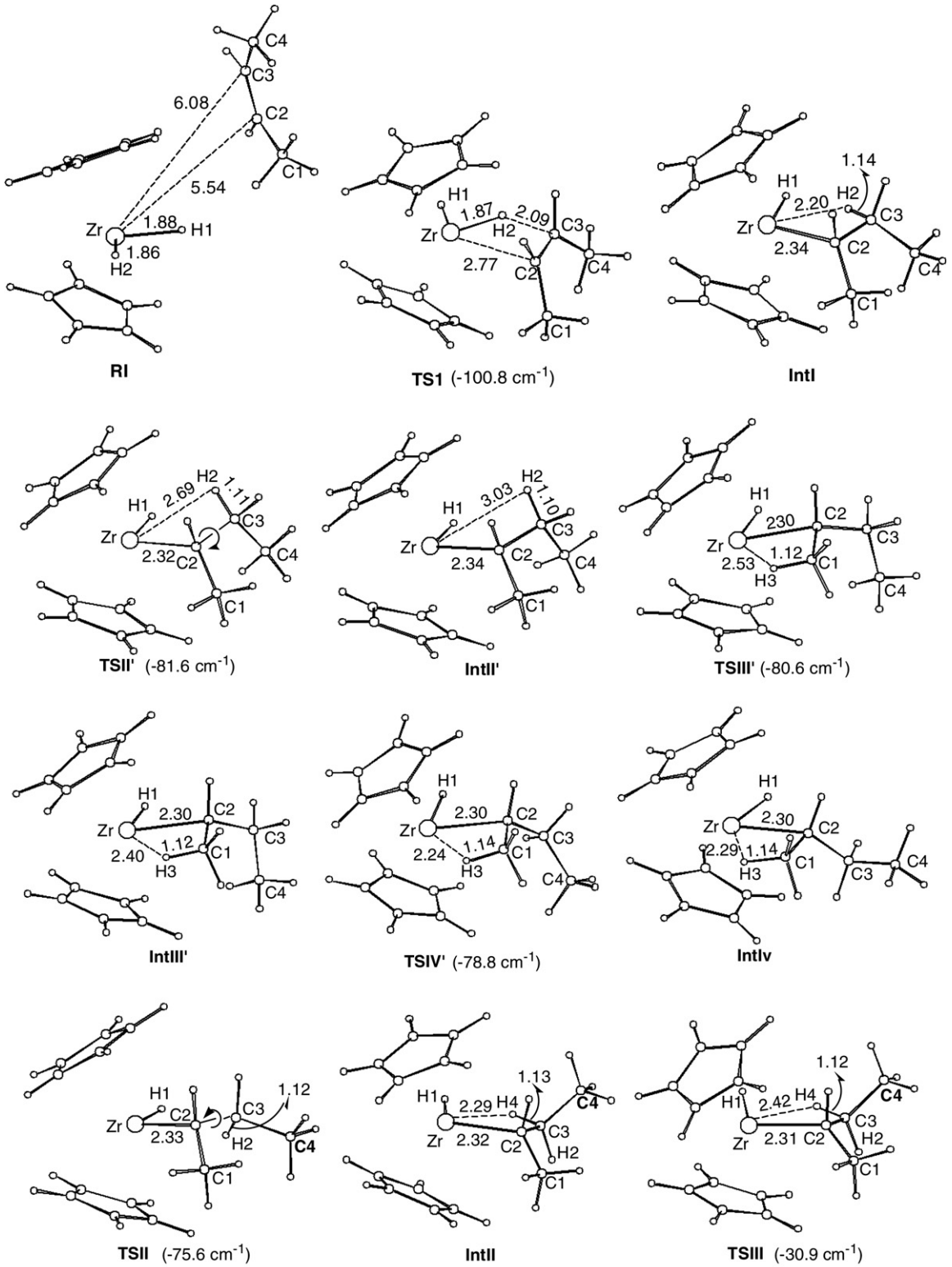

Fig. 2. B3LYP optimized structures for those species shown in Fig. 1 together with selected bond distances. One imaginary frequency for each transition state is given in bracket. The bond distances are given in Å.

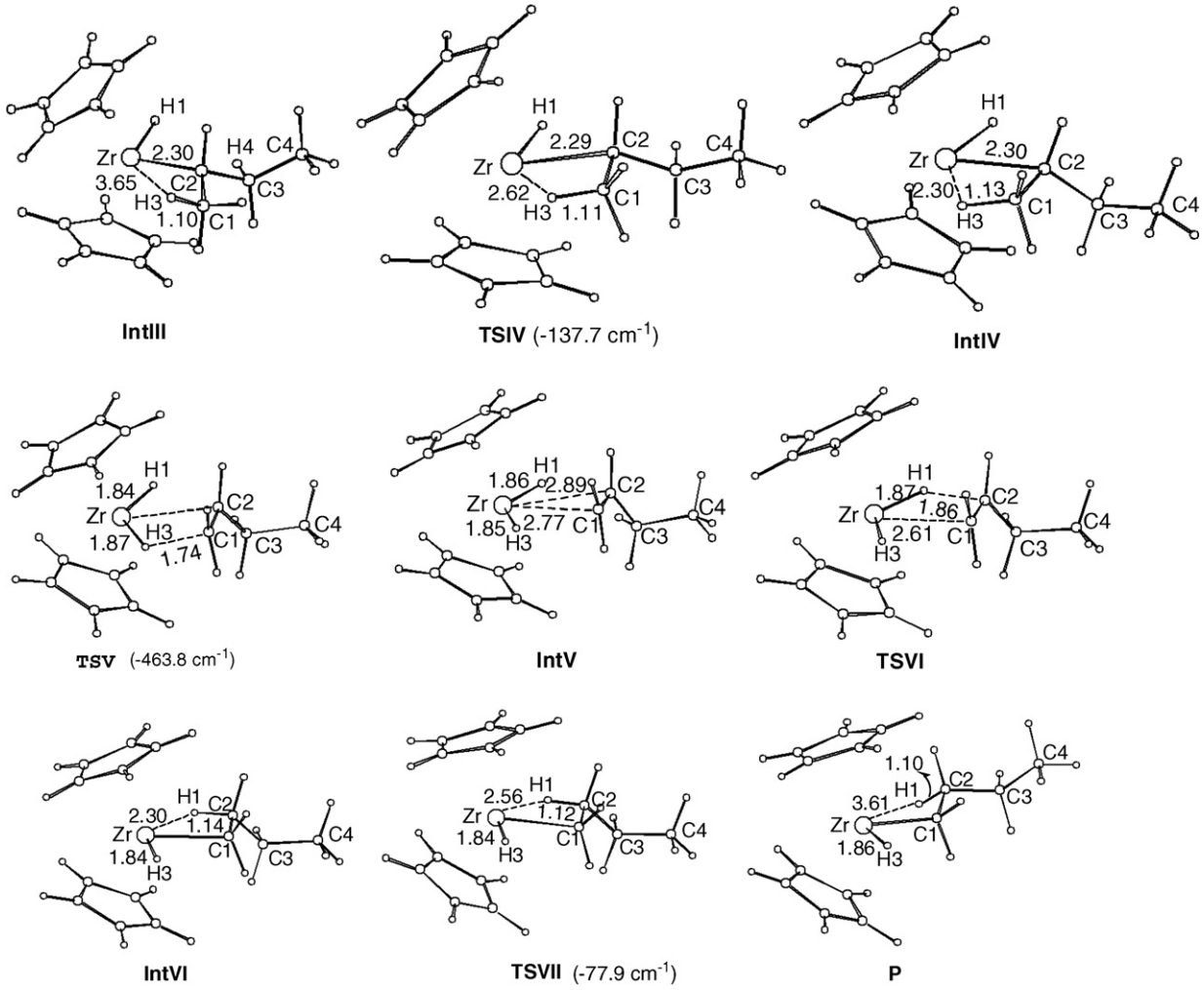

Fig. 2 (*continued*)

the basis sets used in this work have been widely recognized in theoretically investigating structures, bonding and reaction mechanisms of organometallic systems [21,33,34]. Molecular orbitals obtained from the B3LYP calculations were plotted using the MOLDEN v3.5 program written by Schaftenaar [35].

3. Results and discussion

3.1. Mechanistic study on the side-insertion of cis-2-butene into Zr–H bond of Cp_2ZrH_2

The potential energy profile for reaction of Cp_2ZrH_2 with *cis*-2-butene is illustrated in Fig. 1, and the geometrical structures together with selected structural parameters are shown in Fig. 2. The step from **R** to **RI** is only Van der Waals interaction between Cp_2ZrH_2 and the *cis*-2-butene. Step 1 (**RI** to **IntI**) is the side-insertion of *cis*-2-butene into the Zr–H2 to give a metal alkyl hydride intermediate **IntI**. A Zr···H2–C3 central-agostic interaction is involved in the intermediate, supported by the distances of Zr···H2 (2.20 Å), C3–H2 (1.14 Å) and the C3–C2–Zr bond angle (85.9°). This step is quite favorable thermodynamically mainly due to formation of the stable C3–H2 bond. The next step is cleavage of the Zr···H2–C3 agostic interaction by rotating the C2–C3 bond. Obviously, two possible paths can be proposed by defining opposite rotation directions. One path from **Int1** starts with the C2–C3 bond rotation in the direction as illustrated by the bent arrow in **TSII′** (see Fig. 2). From **IntI** to **TSII′**, the Zr···H2–C3 central-agostic interaction is broken with the C2–C3 bond rotation. The Zr–H2 distance increases from 2.20 Å in **IntI** to 3.03 Å in **IntII′** and the C3–H2 returns to the normal bond distance (1.10 Å). The step from **IntII′** to **IntIII′** is formation of a new Zr···H3–C1 side-agostic interaction. **IntIII′** isomerizes to **IntIV** through the C2–C3 bond rotation and the Zr···H3–C1 side-agostic interaction is further strengthened. Another possible pathway from **IntI** starts with the C2–C3 bond rotation in the direction as illustrated by the bent arrow in **TSII** (see Fig. 2). From **IntI** to **IntII**, the Zr···H2–C3 central-agostic interaction is broken and on the meantime, a new Zr···H4–C3 central-agostic interaction is formed with the C2–C3 bond rotation. The step from **IntII** to **IntIII** is a process of weakening the Zr···H4–C3 agostic interaction. The Zr···H4 distance is elongated to 2.73 Å and the H4–C3 bond length is reduced to 1.11 Å, indicative of only weak agostic interaction involved. From **IntIII** to **IntIV**, the weak Zr···H4–C3 central-agostic interaction disappears completely and a Zr···H3–C1 side-agostic interaction is formed, giving the intermediate **IntIV**. The step from **IntIV** to **IntV** is a β-hydrogen elimination reaction in which the hydrogen migrates from C1 to Zr. In **IntV**, one new Zr–H bond is generated and the coordinated 1-butene is formed. The barrier (13.2 kcal/mol) is quite high as a result of breaking the stable C1–H3 bond. **IntV** is much less stable than **IntIV**. Lack of backbonding from the metal to the olefin leads to weak interaction between the fragment Cp_2ZrH_2 and the olefin,

which is responsible for the less stable of **IntV**. Step 6 (**IntV** to **IntVI**) is another olefin insertion where 1-butene inserts into the Zr–H1 bond. **IntVI** is another metal alkyl hydride intermediate with the occurrence of a side-agostic interaction of Zr···H1–C2. Comparison of the structural parameters of **IntVI** with the final product **P** confirmed the claim of the agostic interaction (**P** to **IntVI**: Zr–H1 3.61 Å → 2.30 Å, C2–H1 1.10 Å → 1.14 Å, Zr–C1–C2 126.2° → 89.8°). The kinetic barrier is calculated to be 0.3 kcal/mol, implying the C=C central-insertion is preferred kinetically over the side-insertion. Clearly, **IntVI** is more stable than **IntV** due to formation of the stable C2–H1 bond. In step 7 (**IntVI** to **P**), the side-agostic interaction disappears and **IntVI** isomerizes to the more stable product **P**. **P** is more stable than **IntVI** although **IntVI** involves side-agostic interaction. That is to say, the intermediate with side-agostic interaction is less stable than the one without it. It can be predicted from the energy profile that the

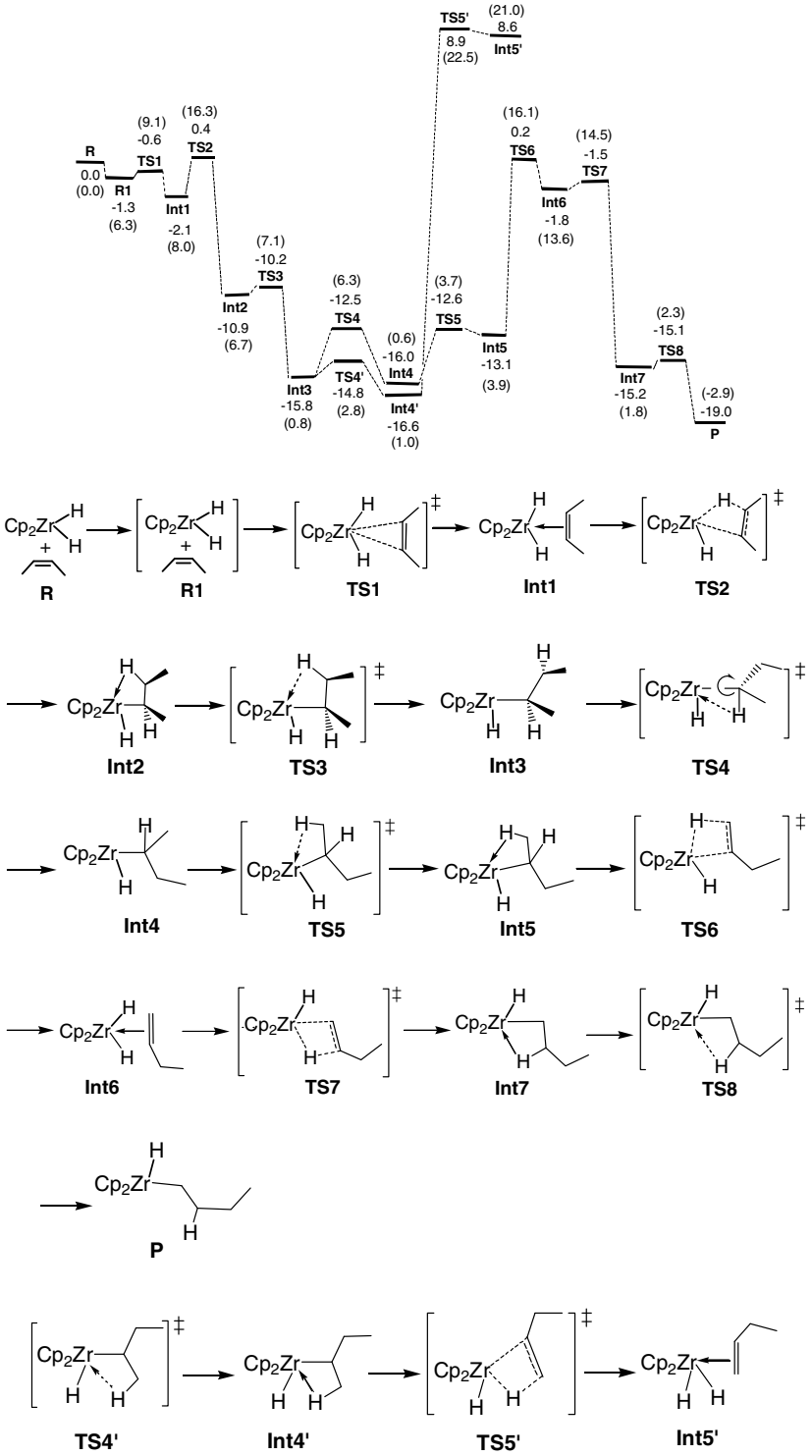

Fig. 3. Potential energy profile for the central-insertion of *cis*-2-butene into the Zr–H of Cp_2ZrH_2. The free energies are given in bracket. The energies are given in kcal/mol.

cis-2-butene insertion is the rate-determining step, and the reaction is favorable thermodynamically. The path through steps 2, 3 and 4 is more favorable kinetically than that through steps 2′, 3′ and 4′.

From the above discussions we can draw conclusions as follows: (i) *cis*-2-butene cannot form a dative bond with the metal center of Cp_2ZrH_2 to afford a stable adduct. (ii) The side-olefin insertion into the Zr–H of Cp_2ZrH_2, giving a metallocene alkyl species, is favorable both kinetically and thermodynamically as demonstrated by steps 1 and 6. Conversely, β-hydrogen elimination, giving a metallocene alkene species, is unfavorable both kinetically and thermodynamically as demonstrated by steps 5 and the reverse of 1 and 6. (iii) Formation of the C–H side-agostic interaction to the metal center makes the metallocene alkyl species less stable relative to those without such agostic interactions as demonstrated in steps 3′, 4 and 7, respectively. (iv) From the pathway discussed above, it can be seen that the typical organometallic reactions, such as olefin insertion, β-hydrogen elimination, agostic interaction and cleavage of the agostic bonding, are the fundamental and indispensable steps for reaction of Cp_2ZrH_2 with *cis*-2-butene.

3.2. Mechanistic study on the central-insertion of cis-2-butene into the Zr–H of Cp_2ZrH_2

In this path, we employ *cis*-2-butene as a substrate to confirm whether the side-insertion or the central-insertion into the Zr–H bond of Cp_2ZrH_2 is preferred kinetically. The potential energy profile for the central-insertion of *cis*-2-butene into the Zr–H of Cp_2ZrH_2 is shown in Fig. 3, and the geometrical structures together with selected structural parameters are illustrated in Fig. 4. **R** to **R1** is just formation of the Van der Waals interaction between Cp_2ZrH_2 and the *cis*-2-butene. **R1** to **Int1** is the central-insertion of the *cis*-2-butene *via* a transition state **TS1**, giving the intermediate **Int1**. The Zr–C2, Zr–C3 distances are calculated to be 2.99 Å, indicating a dative bond between Zr and C2=C3 is formed in **Int1**. This step is quite favorable kinetically as a result of the very low barrier, and is a little favorable thermodynamically as a result of formation of the dative bond. The step from **Int1** to **Int2** is an olefin insertion process. The C2=C3 double bond inserts into the Zr–H2 bond *via* **TS2** to give a metal alkyl hydride intermediate (**Int2**). A side-agostic interaction of Zr···H2–C2 is formed in **Int2**, supported by the following structural data. The Zr–H2, C2–H2 distances and the Zr–C3–C2 bond angle are calculated to be 2.22 Å, 1.15 Å and 87.2°, respectively. The barrier for the step is 2.5 kcal/mol. **Int2** is more stable than **Int1**. The step from **Int2** to **Int3** is cleavage of the agostic interaction of Zr···H2–C2 in which the Zr–H2 increases from 2.22 Å in **Int2**, *via* 2.59 Å in **TS3** to 3.70 Å in **Int3**. At first sight, the following step is firstly the formation of a Zr···H4–C4 central-agostic interaction (**Int3** to **Int4**′), and then followed by the β-hydrogen elimination (**Int4**′ to **Int5**′). The barrier for formation of the central-agostic interaction is relatively low (1.1 kcal/mol), and **Int4**′ has higher stability relative to **Int3**. However, for the step (**Int4**′ to **Int5**′), the results of calculations show that the barrier for the β-hydrogen elimination is significantly high (24.2 kcal/mol).

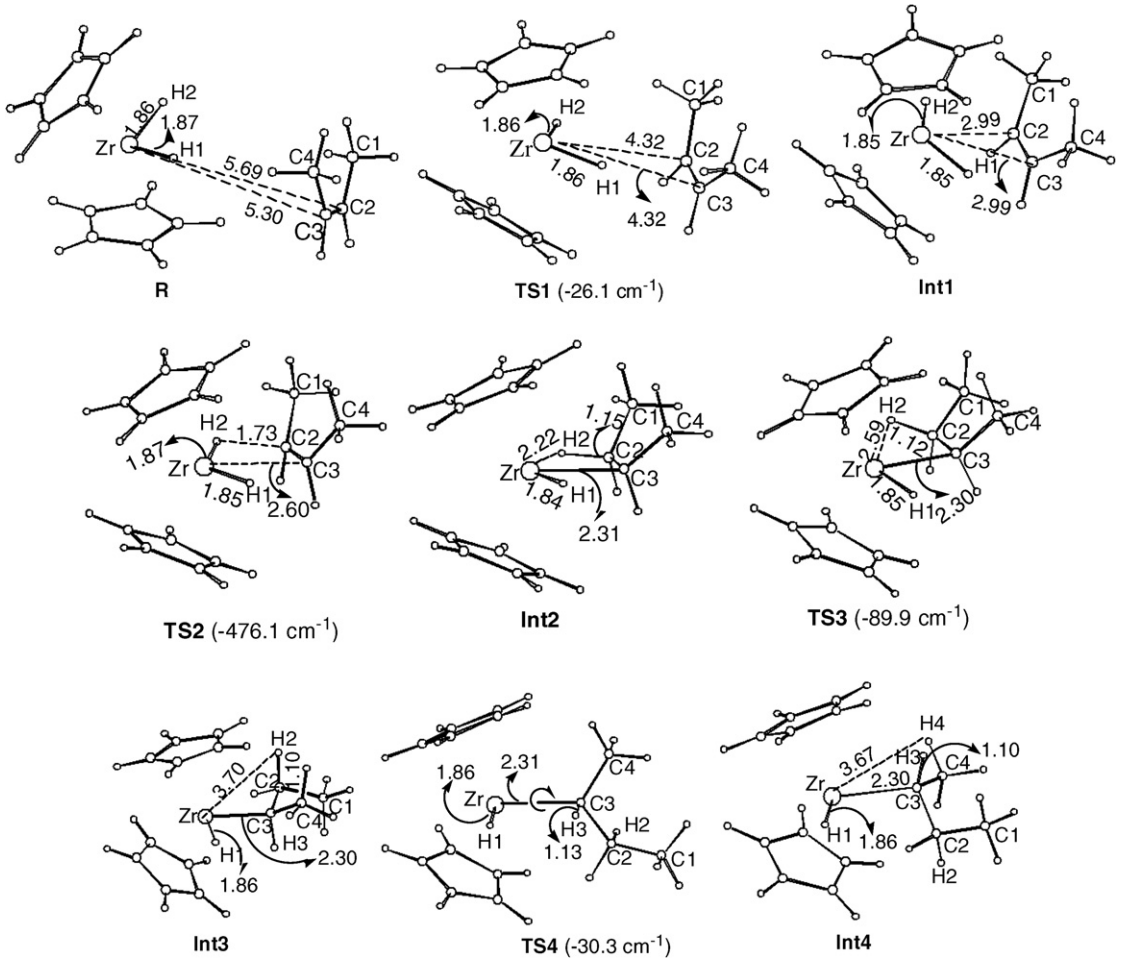

Fig. 4. B3LYP optimized structures for those species shown in Fig. 3 together with selected bond distances. One imaginary frequency for each transition state is given in bracket. The bond distances are given in Å.

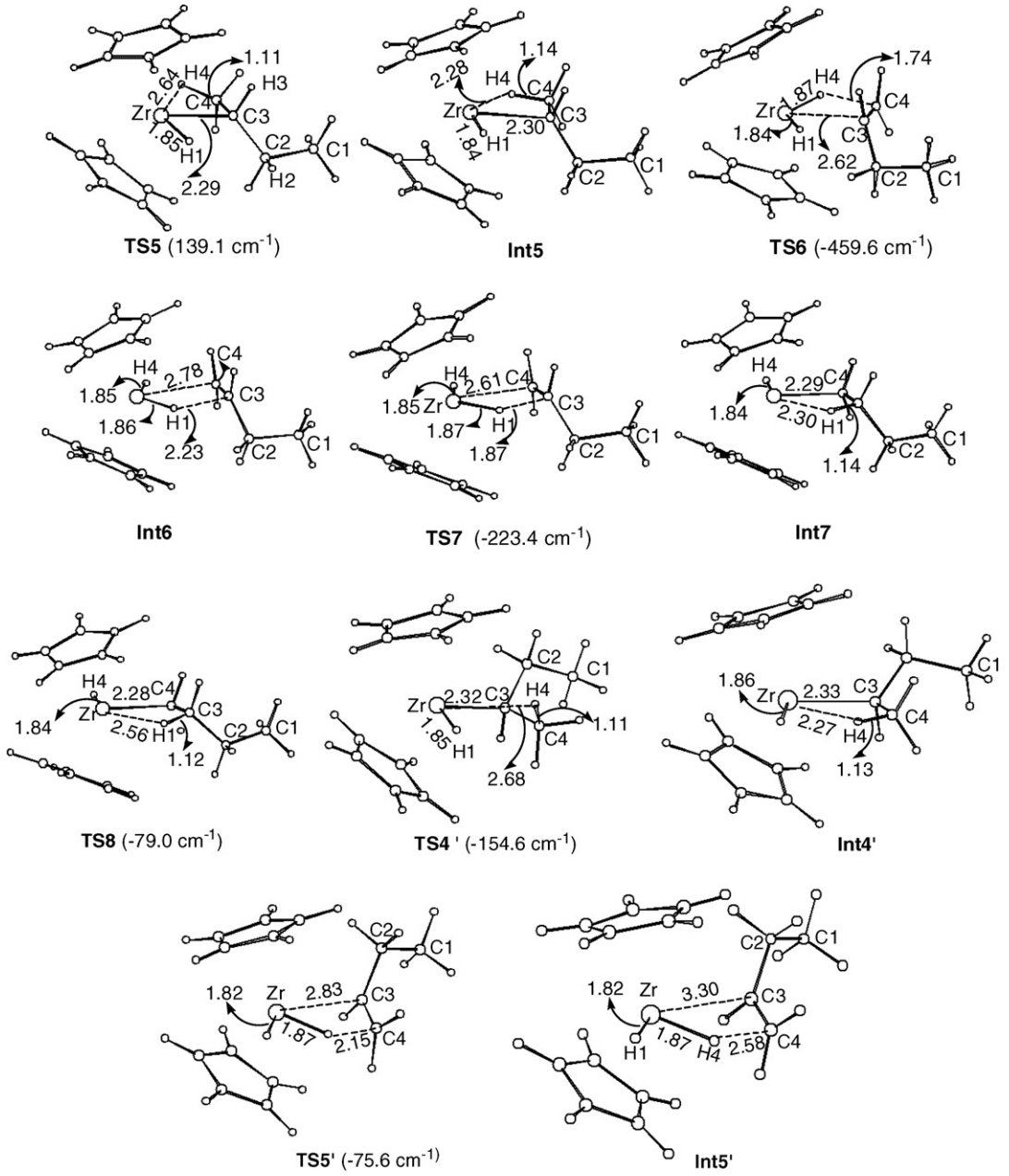

Fig. 4 (*continued*)

This step is analogous to the one from **IntIV** to **IntV** shown in Fig. 1, but the barrier from **Int4′** to **Int5′** is obviously higher than that for the step from **IntIV** to **IntV** (13.2 kcal/mol). This is apparently associated with the much less stability of **Int5′** compared to **IntV**. The instability of **Int5′** arises from the strong steric hindrance between one Cp and the ethyl attached on the C3 atom. The high barrier for the step implies this pathway is disfavored kinetically, and also, inspires us to explore another possible pathway. Fortunately, a species (**Int6**) analogous to **IntV**, where the C=C bond lies in between the two Zr–H bonds, can be obtained from **Int3** through Zr–C3 σ-bond rotation and the subsequent steps, as proposed in Fig. 3. The step from **Int3** to **Int4** is a Zr–C3 σ-bond rotation as shown by the bent arrow in **TS4**. By σ-bond rotation, the ethyl attached to C3 becomes close to H1, and the methyl attached to C3 goes far away from H1. Interestingly, a Zr···H3–C3 agostic interaction is involved in **TS4**, while the two intermediates connected by **TS4** do not involve such kind of interactions. The distances of Zr–H3 (2.36 Å), C3–H3 (1.13 Å) and the Zr–C3–H3 bond angle (78.8°) support the occurrence of the agostic interaction in **TS4**. As is known, the three frontier orbitals of the Cp_2M moiety lie in the plane which partitions the two Cp rings as illustrated below [11].

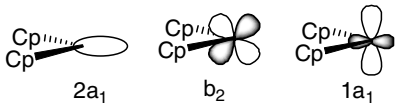

As a result, only the C3–H3 bond lies in the H1–Zr–C3 plane, can the d orbital of the metal have the same symmetry with the C3–H3 bonding orbital and the antibonding orbital, making the agostic interaction take effect. In **Int3** and **Int4**, the H1–Zr–C3–H3 dihedral angles are 71.6° and −72.7°, respectively, indicating the C3–H3 bond lies obviously off the H1–Zr–C3 plane. Therefore, no agostic interaction is involved in both intermediates. As for **TS4**, the

H1–Zr–C3–H3 dihedral angle is only 0.1°, indicating the C3–H3 bond lies essentially in the H1–Zr–C3 plane and therefore confirming the occurrence of the agostic interaction. The step from **Int4** to **Int5** is formation of an agostic interaction of Zr with H4–C4. The Zr–H4 and C4–H4 distances, and Zr–C3–C4 angle change from 3.67 Å to 2.28 Å, 1.10 Å to 1.14 Å, 127.7° to 87.7°, respectively. Following this step, **Int5** undergoes a process of β-hydrogen elimination giving **Int6**. In this step, H4 migrates to the metal center from C4, forming a hydride and a coordinated 1-butene ligand. **Int6** is analogous to **IntV** in Fig. 1. Then, the C=C bond of 1-butene inserts into Zr–H1 to afford a metal *n*-alkyl hydride intermediate (**Int7**) accompanying occurrence of the Zr···H1–C3 side-agostic interaction. The last step (**Int7** to **P**) is cleavage of the Zr···H1–C3 side-agostic interaction. The reason why **P** serves as final product while not the **Int7** is that **P** is obviously more stale than **Int7**. As a result, the pathway involving the Zr–C3 σ-bond rotation is preferred kinetically. The *cis*-2-butene insertion (**Int1** to **Int2**) is predicted to be the rate-determining step owing to the highest kinetic barrier (0.4 kcal/mol) relative to **R**. The structural difference between **IntIV** to **P** and **Int5** to **P** is that the H and the ethyl attached on β-carbon atom are exchanged mutually.

What is drawn by examining all the two energy profiles (Figs. 1 and 3) is as follows:

(i) An adduct can be formed by the olefin coordination to the metal center from the central position, and cannot be formed from the outside of the Zr–H bond. This also implies the attack of *cis*-2-butene from the central position might be more favorable. For example, **RI** in Fig. 1 is not an adduct, because no olefin-to-metal dative bond can be formed. **IntV** in Fig. 1 and **Int1** in Fig. 3 are adducts because the olefin-to-metal dative bond is afforded. This can be rationalized by using the LUMO of Cp_2ZrH_2. As shown in Scheme 3, the overlap of between the LUMO of Cp_2ZrH_2 and the π bonding orbital of olefin is more effective from the central position than from the outside of the Zr–H bond.

(ii) As is known, agostic C–H–M interactions are potentially significant structural characters of unsaturated metal complexes that are intermediates in olefin polymerization, C–H activation, and other metal-mediated or -catalyzed reactions [36]. It has been proposed by Rooney, Brookhart and Green [37] that insertion of olefins into the metal–alkyl bond of a Ziegler–Natta catalyst might require an agostic interaction with the metal center [38]. For the systems studies here, it has been confirmed whether formation or the cleavage of C–H agostic interaction to the metal center is indispensable steps for the isomerization of a metallocene *sec*-alkyl hydride to a metallocene *n*-alkyl hydride.

In addition, we found that the species with side-agostic or central-agostic interaction have different stability. The species with side-agostic is less stable than without it, and the species with central-agostic is more stable than without it. For example, the relative stability related to the central-agostic is: **IntI** > **IntII′**, **IntII** > **IntIII** (Fig. 1), and the relative stability related to the side-agostic is: **IntVI** < **P**, **IntIV** < **IntIII**, **IntIII′** < **IntII′** (Fig. 1); **Int2** < **Int3**, **Int5** < **Int4**, **Int7** < **P** (Fig. 3). Based on the above observations, we can qualitatively describe that the path through steps 2, 3 and 4 is preferred over the path through steps 2′, 3′ and 4′ in Fig. 1. **IntI** to **IntII′** undergoes a cleavage of central-agostic, and **IntII′** to **IntIII′** undergoes a formation of side-agostic process. Both steps are endothermic. **IntI** to **IntII** undergoes from a central-agostic to a new central-agostic process. **IntII** is more stable than **IntI**, probably due to the less steric hindrance involved in **IntII**.

(iii) Olefin insertion into the Zr–H of Cp_2ZrH_2 is favored (such as **RI** to **IntI**, **Int1** to **Int2**, and **Int6** to **Int7**), while β-elimination is disfavored both kinetically and thermodynamically (such as **IntIV** to **IntV**, and **Int5** to **Int6**). The exothermic process of olefin insertion is the driving force for the reaction of Cp_2ZrH_2 with *cis*-2-butene.

(iv) It is predicted by our results of calculations that the pathway involving the central-insertion is preferred because this pathway has a kinetic barrier of only 0.4 kcal/mol. The pathways involving the side-insertion of *cis*-2-butene have the barrier of above 6 kcal/mol, indicating disfavored kinetically. The preference for the pathway involving the central-insertion can be rationalized in terms of MO analysis of Cp_2ZrH_2, so called the fragment molecular orbital approach considering symmetry and energy requirements for the possible donation. The lowest unoccupied molecular orbital (LUMO) for Cp_2ZrH_2 is shown in Scheme 3. For the central-insertion, the bonding π orbital of the olefin can effectively overlap with the LUMO of Cp_2ZrH_2. For the side-insertion, the bonding π orbital of the olefin cannot effectively overlap with the LUMO of Cp_2ZrH_2 compared to the case of central-insertion. In addition, we calculated the deformation energies for **TSI** and **TS2** (Scheme 4). **TSI-a** and **TSI-b** are directly derived from **TSI**, and **TS2-a** and **TS2-b** are directly derived from **TS2**. $E_{binding}$ and $E'_{binding}$ are the binding energy between **TSI-a** and **TSI-b** and between **TS2-a** and **TS2-b**, respectively. It can be seen from Scheme 4 that the activation energy difference is mainly resulted from the different deformation of **TSI-a** and **TS2-a**. This means the deformation energy of Cp_2ZrH_2 is an important factor. What needs to say here is that the IRC identification in locating the variety of intermediates plays an important role.

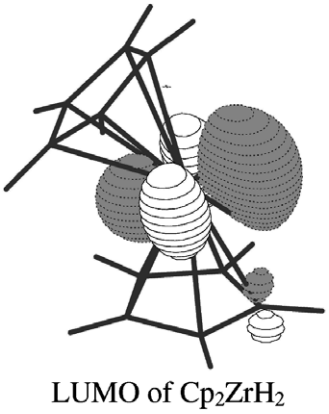

Scheme 3.

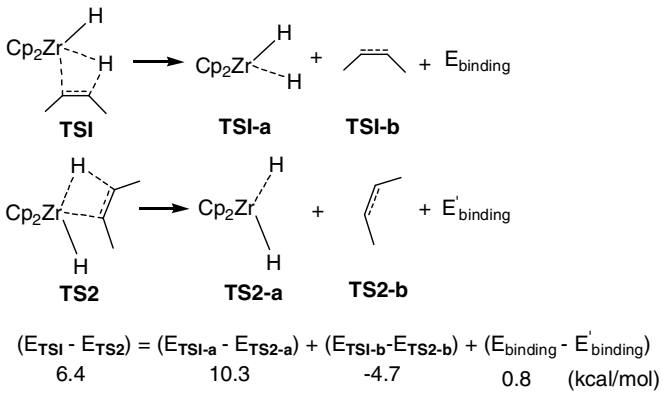

Scheme 4.

4. Conclusions

On the basis of the experimental observations by Chirik and Bercaw that Cp_2ZrH_2 reacts with *cis*-2-butene to yield a metal *n*-butyl hydride product, we theoretically explored the detailed mechanisms for the kind of reactions with the aid of density functional theory calculations. There two possible pathways for insertion of *cis*-2-butene. One is the side-insertion, and another is the central-insertion. Compared with the side-insertion, the central-insertion is predicted to be more favorable kinetically, which can be explained through the fragment molecular orbital approach.

The reaction of Cp_2ZrH_2 with *cis*-2-butene undergoes two processes. One is the olefin insertion to give a metallocene *sec*-butyl hydride intermediate, and the other following this step is the isomerization of the intermediate to the final product, a metallocene *n*-butyl hydride. Investigation of the detailed reaction mechanisms reveals, with the help of the IRC identification, that formation and cleavage of agostic interaction, β-hydrogen elimination are the requisite steps in addition to the olefin insertion. Calculated results showed that insertion of olefin into the Zr–H of Cp_2ZrH_2 is more favorable both thermodynamically and kinetically than its reverse process, the β-hydrogen elimination, which gives the driving force for olefin insertion reactions. It is found two kinds of agostic interactions involved in the metallocene butyl hydride intermediates. The metal alkyl hydride with the central-agostic binding is more stable than without it, and those with the side-agostic binding is less stable than without it, which plays a role in describing which path is preferred.

Acknowledgement

This work was supported by the Nature Science Foundation of Shandong Province (No. Y2007B23).

References

[1] D.E. Richardson, N.G. Alameddin, M.F. Ryan, T. Hayes, J.R. Eyler, A.R. Siedle, J. Am. Chem. Soc. 118 (1996) 11244.
[2] P.C. Mohring, N.J. Coville, J. Organomet. Chem. 479 (1994) 1.
[3] A.M. Thayer, Chem. Eng. News 73 (37) (1995) 15.
[4] N.M. Doherty, J.E. Bercaw, J. Am. Chem. Soc. 107 (1985) 2670.
[5] G.W. Parshall, Homogeneous Catalysis, John Wiley & Sons, New York, 1980 (Chapter 3).
[6] R.J. Cross, The Chemistry of the Metal–Carbon Bond, Vol. 2, John Wiley & Sons, New York, 1985 (Chapter 8).
[7] P.L. Watson, J. Am. Chem. Soc. 104 (1982) 337.
[8] G.W. Parshall, Homogeneous Catalysis, John Wiley & Sons, New York, 1980 (Chapters 3–5).
[9] P.J. Chirik, J.E. Bercaw, Organometallics 24 (2005) 5407.
[10] J.L. Petersen, L.F. Dahl, J. Am. Chem. Soc. 97 (1975) 6416. 6422.
[11] J.W. Lauher, R. Hoffmann, J. Am. Chem. Soc. 98 (1976) 1729.
[12] J.C. Green, Chem. Soc. Rev. 27 (1998) 263.
[13] G. Erker, F. Rosenfeldt, Angew. Chem. 90 (1978) 640.
[14] G. Erker, F. Rosenfeldt, Angew. Chem. Int. Ed. Engl. 17 (1978) 605.
[15] G. Erker, F. Rosenfeldt, J. Organomet. Chem. 188 (1980) C1.
[16] G. Erker, Acc. Chem. Res. 17 (1984) 103.
[17] G. Fachinetti, F.C. loriani, F. Marchetti, S. Merlino, J. Chem. Soc., Chem. Commun. (1976) 522.
[18] G. Fachinetti, G. Fochi, C. Floriani, J. Chem. Soc., Dalton Trans. (1977) 1946.
[19] G. Fachinetti, C. Floriani, H. Stoeckli-Evans, J. Chem. Soc., Dalton Trans (1977) 2297.
[20] S.A. Cummings, R. Radford, G. Erker, G. Kehr, R.F. Hlich, Organometallics 25 (2006) 839.
[21] L.A. Watson, D.V. Yandulov, K.G. Caulton, J. Am. Chem. Soc. 123 (2001) 603.
[22] J. Endo, N. Koga, K. Morokuma, Organometallics 12 (1993) 2777.
[23] C. Lee, W. Yang, G. Parr, Phys. Rev. B 37 (1988) 785.
[24] B. Miehlich, A. Savin, H. Stoll, H. Preuss, Chem. Phys. Lett. 157 (1989) 200.
[25] A.D. Becke, J. Phys. Chem. 98 (1993) 5648.
[26] P.J. Hay, W.R. Wadt, J. Chem. Phys. 82 (1995) 299.
[27] J. Andzelm, S. Huzinaga, Gaussian Basis Sets for Molecular Calculations, Elsevier Science, New York, 1984.
[28] M.S. Gordon, Chem. Phys. Lett. 76 (1980) 163.
[29] R.C. Binning, L.A. Curtiss, J. Comput. Chem. 11 (1990) 1206.
[30] K. Fukui, J. Phys. Chem. 74 (1970) 4161.
[31] K. Fukui, Acc. Chem. Res. 14 (1981) 363.
[32] M.J. Frisch, G.W. Trucks, H.B. Schlegel, G.E. Scuseria, M.A. Robb, J.R. Cheeseman, V.G. Zakrzewski, J.A. Montgomery, Jr., R.E. Stratmann, J.C. Burant, S. Dapprich, J.M. Millam, A.D. Daniels, K.N. Kudin, M.C. Strain, O. Farkas, J. Tomasi, V. Barone, M. Cossi, R. Cammi, B. Mennucci, C. Pomelli, C. Adamo, S. Clifford, J. Ochterski, G.A. Petersson, P.Y. Ayala, Q. Cui, K. Morokuma, D.K. Malick, A.D. Rabuck, K. Raghavachari, J.B. Foresman, J. Cioslowski, J.V. Ortiz, B.B. Stefanov, G. Liu, A. Liashenko, P. Piskorz, I. Komaromi, R.Gomperts, R.L. Martin, D.J. Fox, T. Keith, M.A. Al-Laham, C.Y. Peng, A. Nanayakkara, C. Gonzalez, M. Challacombe, P.M.W. Gill, B.G. Johnson, W. Chen, M.W. Wong, J.L. Andres, M. Head-Gordon, E.S. Replogle, J.A. Pople, GAUSSIAN 98, Revision A.9, Gaussian Inc., Pittsburgh, PA, 1998.
[33] (a) S. Bi, Z. Lin, R.F. Jordan, Organometallics 23 (2004) 4882;
(b) S. Bi, A. Ariafard, G. Jia, Z. Lin, Organometallics 24 (2005) 680;
(c) A. Ariafard, S. Bi, Z. Lin, Organometallics 24 (2005) 2241;
(d) A. Ariafard, Z. Lin, Organometallics 24 (2005) 3800.
[34] (a) S. Bi, S. Zhu, Z. Zhang, Z. Yuan, J. Organomet. Chem. 692 (16) (2007) 3454;
(b) S. Bi, S. Zhu, Z. Zhang, Eur. J. Inorg. Chem. 14 (2007) 2046;
(c) S. Bi, Z. Zhang, S. Zhu, Chem. Phys. Lett. 431 (2006) 385;
(d) S. Bi, B. Wang, Y. Zhao, Z. Zhang, S. Zhu, Chem. Phys. Lett. 426 (2006) 192;
(e) X. Zhu, B. Zhao, B. Wang, Y. Zhao, S. Bi, Chem. Phys. Lett. 422 (2006) 6.
[35] G. Schaftenaar, MOLDEN v3.5, CAOS/CAMM Center Nijmegen, Toernooiveld, Nijmegen, The Netherlands, 1999.
[36] (a) M. Brookhart, M.L.H. Green, L. Wong, Prog. Inorg. Chem. 36 (1988) 1;
(b) R.H. Crabtree, D.G.Adu. Hamilton, Organomet. Chem. 28 (1988) 299.
[37] (a) D.T. Laverty, J.J. Rooney, J. Chem. Soc., Faraday Trans. 79 (1983) 869;
(b) M. Brookhart, M.L.H. Green, J. Organomet. Chem. 250 (1983) 395;
(c) M. Brookhart, M.L.H. Green, L. Wong, Prog. Inorg. Chem. 36 (1988) 1.
[38] (a) This proposal has been supported by theoretical studies H. Kawamura-Kunbayashi, N. Koga, K. Morokuma, J. Am. Chem. Soc. 114 (1992) 8687;
(b) L.A. Castonguay, A.K. RappB, J. Am. Chem. Soc. 114 (1992) 5832;
(c) M.H. Prosenc, C. Janiak, H.H. Brintzinger, Organometallics 11 (1992) 4036;
(d) T.K. Woo, L. Fan, T. Ziegler, Organometallics 13 (1994) 432;
(e) H. Weiss, M. Ehrig, R. Ahlrichs, J. Am. Chem. Soc. 116 (1994) 4919.